CHEMISTRY
A European Journal

A Journal of
ChemPubSoc Europe

Accepted Article

Title: Electrochemical and scalable dehydrogenative C(sp3)-H amination via remote hydrogen atom transfer in batch and continuous flow

Authors: Pavlo Nikolaienko, Marc Jentsch, Ajit Prabhakar Kale, and Magnus Rueping

To be cited as: *Chem. Eur. J.* 10.1002/chem.201806092

Link to VoR: http://dx.doi.org/10.1002/chem.201806092

Supported by
ACES

WILEY-VCH

10.1002/chem.201806092

WILEY-VCH

Electrochemical and scalable dehydrogenative C(sp^3)-H amination via remote hydrogen atom transfer in batch and continuous flow

Pavlo Nikolaienko,[a] Marc Jentsch,[b] Ajit P. Kale,[a] Yunfei Cai,[a] and Magnus Rueping* [a],[b]

Abstract: A hydrogen atom transfer-directed electrochemical intramolecular C-H amination has been developed in which the N-radical species are generated at the anode, and the base required for the reaction is generated at the cathode. A broad range of valuable pyrrolidines were prepared in good yields and with high chemoselectivity. The reaction was easily scaled up in both batch and continuous flow systems.

Introduction

The implementation of sustainability principles to organic synthesis led to the search for new synthetic methods that require fewer reaction steps, consume less energy and generate less waste and thus have minimal environmental impact. In this regard, the direct functionalization of C-H bonds is highly desirable due to the ubiquity of these bonds in organic compounds. Over the last decade, hydrogen atom transfer (HAT) reactions[1] have attracted considerable attraction as a radical-based strategy[2] and as a good alternative to transition-metal-catalyzed C-H activation methods. HAT reactions typically proceed under milder reaction conditions, and regio-, chemo- and stereoselectivity issues are typically solved either by the presence of N-, O- or C-containing functional groups or by the electronic properties of the substrates.[1]

Poly-substituted 5-membered saturated aza-heterocycles, particularly pyrrolidines, are a frequent structural motif in natural[3] (Figure 1A) and synthetic biologically active compounds[4] (Figure 1B) with a wide range of activities, including antidiabetic, antitumor and anti HIV properties. For example, five of the eight anti-infective drugs approved in 2016, including an antihepatitis C drug, contain a pyrrolidine moiety.[5] Therefore, the development of new and efficient methods to build up these structural entities is of great importance.

The Hofmann-Löffler-Freytag (HLF) reaction[6] is a HAT-based direct amination of poorly reactive alkyl C(sp^3)-H bonds. Through a C-H halogenation-nucleophilic substitution sequence, primary and secondary aliphatic amines are converted into valuable pyrrolidines in a single step.[7] Since the initial reports of the thermal transformation of N-halogenated aliphatic amines to pyrrolidines in the presence of strong acids, the general strategy has remained the same; however, many improvements have been achieved. Recent advances have been reported by Suárez, who showed that the reaction also proceeds under milder neutral conditions with UV light irradiation in the presence of I_2 and lead acetate[8] or a hypervalent iodine reagent I(III).[9] Significant advances were achieved by the Muniz[10] and Nagib[11] groups who reported improved protocols based on I_2 or $I^-(I_3^-)$ and hypervalent iodine I(III) oxidative systems for the light-mediated conversion of sulfonamide-protected amines to the corresponding pyrrolidines.

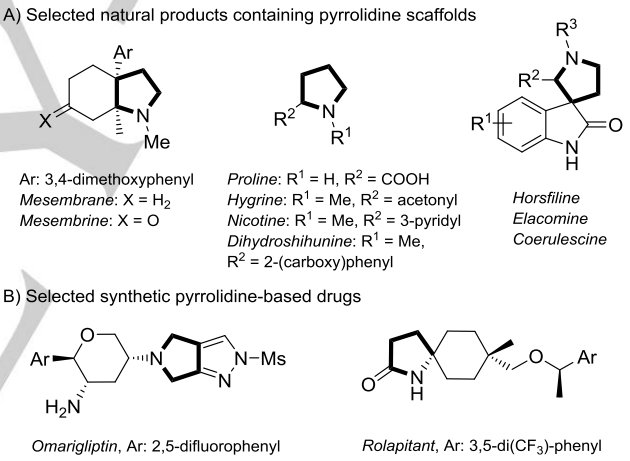

Figure 1. Biologically active pyrrolidines.

Despite these great achievements, most of the reported protocols require halogenated solvents and either prefunctionalized starting materials or a (super)stoichiometric oxidant. Organic electrochemistry has attracted increasing attention over the last few years, mainly due to the replacement of reducing and oxidizing reagents by "traceless" electrons at the cathode and holes at the anode.[12] From a practical perspective, organic electrosynthesis can minimize total energy losses and reduce waste formation, and as a result, these techniques will decrease the overall costs of industrial synthesis.[13] Because N-radicals can be produced electrochemically, as has been demonstrated by Shono and others[14] we aimed to combine such a strategy with a subsequent 1,5-HAT (1,5-hydrogen atom transfer) to circumvent known obstacles related to C(sp^3)-H amination (HLF reaction) and make the developed protocol applicable to large-scale synthetic applications (Scheme 1).

[a] Dr. P. Nikolaienko, Dr. A. P. Kale, Dr. Y. Cai, Prof. Dr. M. Rueping
KAUST Catalysis Center (KCC)
King Abdullah University of Science and Technology (KAUST)
Thuwal 23955-6900, Saudi Arabia
[b] M.Sc. M. Jentsch, Prof. Dr. M. Rueping
Institute of Organic Chemistry, RWTH-Aachen University
Landoltweg 1, 52074 Aachen (Germany)
E-mail: Magnus.Rueping@rwth-aachen.de

Supporting information for this article is given via a link at the end of the document.

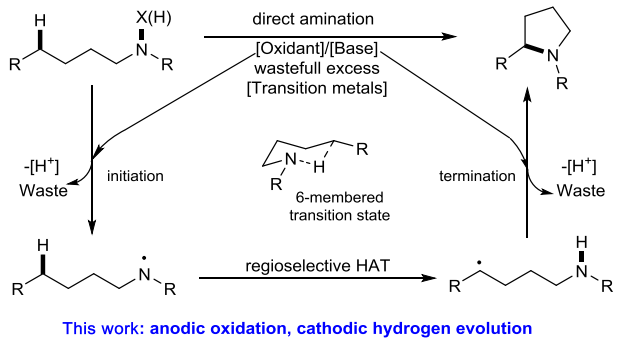

Scheme 1. Regioselective intramolecular C(sp^3)-H bond amination.

Results and Discussion

For initial optimization experiments, the use of precious metal electrodes, such as platinum and gold, as well as the construction of complicated divided cells were not considered due to our intention to scale-up the reaction. Additionally, only methanol and acetonitrile were considered as potential solvents due to industrial green chemistry concerns and proper electrochemical windows.[15] Substrate **1a** was chosen as a model compound and was subjected to direct oxidation in acetonitrile with different tetraalkylammonium salts as the supporting electrolyte (see SI for details).

Table 1. Optimization of the reaction conditions.

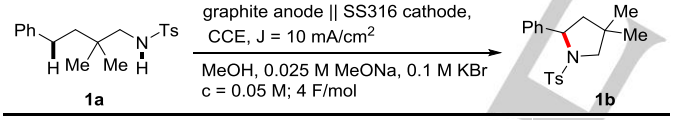

1a **1b**

Entry	Deviation of the reaction conditions[a]	Yield[b]
1	no mediator, MeONa (5 equiv.)	71[c]
2	Pyridine (2 equiv.)	17
3	TFA (10 equiv.)	11
4	Bu_4NPF_6 0.1 M, N- or O-mediators[d] (1 equiv.)	< 10
5	Bu_4NPF_6 0.1 M, ferrocene (1.0 equiv.)	< 5
6	no light or 18W CFL	71 / 74
7	under argon or under air	70 / 72
8	–10 °C or 50 °C	62 / 69
9	Pt anode	19
10	Cu cathode	< 5
11	0.1 M KCl	54
12	0.1 M KI	14
13	CH_3CN/H_2O, NaOH (5 equiv.)	44
14[e]	CH_3CN/H_2O, 0.1 M KBr	68

[a] Reactions were conducted on a 0.2 mmol scale; [b] Yields are based on NMR or GC; [c] Yields strongly vary due to graphite source; [d] Triethylamine, quinuclidine, DABCO, TEMPO, NHPI and HOBt. [e] 8 F/mol.

Electrodes such as graphite, RVC and platinum (for reference) with a wide range of current densities (0.5–50 mA/cm^2) did not generate the desired product with various anode/cathode combinations (see SI). Either recovered starting material or inseparable mixtures of decomposition products were observed in these cases. Among the various tested additives (see SI), bases had a strong impact on the reaction, and the desired product **1b** was finally obtained in decent yield. Encouraged by these findings, we performed extensive screenings of a variety of additives, bases, substrate concentrations, electrode materials and current densities (see SI). To our delight, a 0.025 M solution of **1a** in methanol with 5 equivalents of sodium methoxide, a graphite electrode couple and a current density of 10 mA/cm^2 gave the best result. The desired pyrrolidine **1b** was isolated in 71% yield (Table 1, entry 1), with the deaminated aliphatic aldehyde as the only major byproduct. Not surprisingly, when various graphite sources were tested to evaluate the reproducibility, a strong dependence on the graphite source was observed. The yield of **1b** varied from 40 to 75% under identical reaction conditions. Less absorbing glassy carbon and RVC did not provide reproducible results.

To get an insight into the reaction and understand the reactivity, the electrochemical behavior of the reactants and reagents was investigated. Based on cyclic voltammetry (CV), the redox-potentials of starting materials similar to **1a** were found to be controlled by the outer-sphere oxidation of the nitrogen centered lone pair (see SI) and are all of E_{Red} = 2.0 V vs Ag/Ag^+ and higher. Only substrates possessing electron-rich aromatic substituents showed oxidation peaks from E_{Red} = 1.5 V to E_{Red} = 1.9 V vs Ag/Ag^+ most likely due to oxidation of the benzylic C-H bonds. The E_{Red} of the corresponding product **1b** was found to be very similar to that of the corresponding starting material **1a** [E_{Red}**1a** = 1.9 V vs Ag/Ag^+; E_{Red}**1b** = 2.2 V vs Ag/Ag^+] (Figure 2). This observation support the failed attempts on direct amination either due to poor reactivity or by overoxidation.

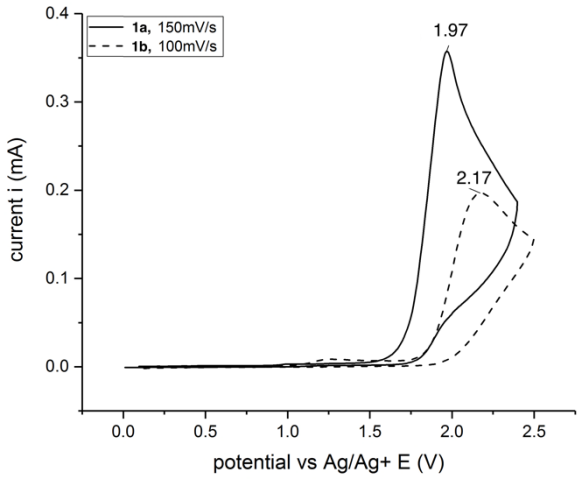

Figure 2. Cyclic voltammetry of the **1a** (solid line) and **1b** (dashed line) (5 mM in 0.1 M of Bu_4NPF_6 in CH_3CN); Work. el.: glassy carbon, 8 mm^2; Ref. el.: Ag-wire in 10 mM $AgNO_3$ / 0.1 M Bu_4NPF_6 in CH_3CN.

According to our design, the desired C-H amination is expected to be initiated by the formation of N-centered radicals. Thus, the effect of different protecting groups was tested. When an unprotected amine was subjected to the reaction conditions, the corresponding deaminated aldehyde was isolated as the sole product. Acetyl-based protecting groups such as trifluoroacetyl and benzoyl as well as phosphamide did not provide any product over the course of the reaction. Only tosyl-protected amines were able to provide the desired product. Subsequently, CV-studies were performed with amine **26A** which bears different protecting groups and has no aromatic residue on the aliphatic chain (Figure 3). As expected, the E_{Red} potential was found to be dependent on the nature of the protecting group and only substrates with protecting groups incorporating aromatic rings (Ts, Bz, $PO(OPh)_2$) featured a redox-potential E_{Red} in the range of 2.0 V vs Ag/Ag^+.

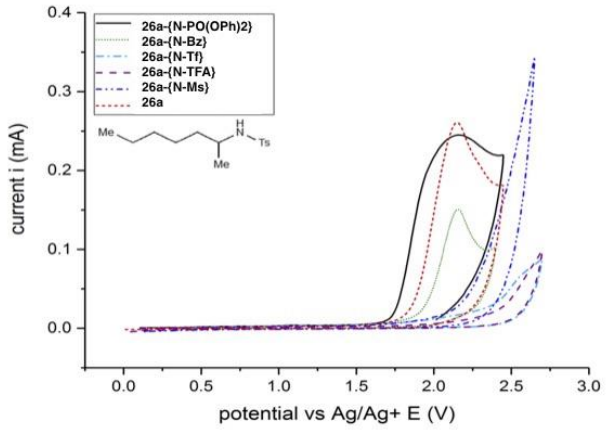

Figure 3. Protection group effect on **26A** (5 mM in 0.1 M of Bu_4NPF_6 in CH_3CN); Work. el.: glassy carbon, 8 mm^2; Ref. el.: Ag-wire in 10 mM $AgNO_3$ / 0.1 M Bu_4NPF_6 in CH_3CN; scan rate = 100 mV/s.

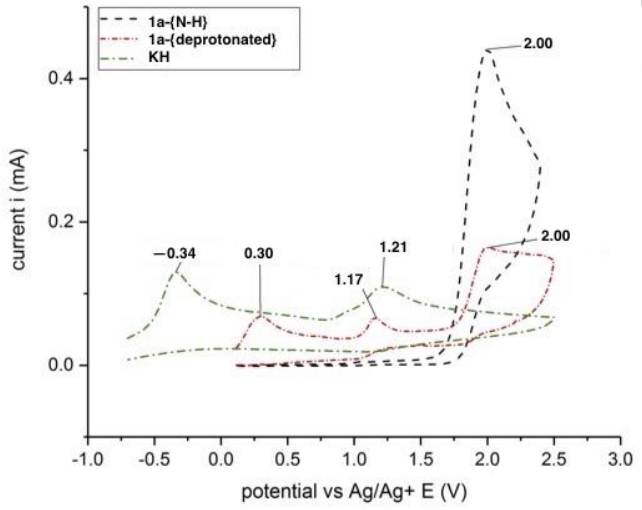

Figure 4. Cyclic voltammetry of the protonated **1a** (dashed line), deprotonated **1a** (potassium salt; dash-dotted red line) and of the slurry of potassium hydride (dash-dotted line green). All substances of 5 mM in 0.1 M of Bu_4NPF_6 in CH_3CN); Work. el.: glassy carbon, 8 mm^2; Ref. el.: Ag-wire in 10 mM $AgNO_3$ / 0.1 M Bu_4NPF_6 in CH_3CN; scan rates = 100 mV/s.

Despite similarities in the redox-potential of benzoyl, phosphoryl and tosyl-protected amines, only the latter was converted into the corresponding product under the given conditions, most probably due to much higher acidity of the N-H bond. Indeed, the redox-potential of deprotonated **1a** is almost 1.5 V lower (E_{Red}**1a**$^-K^+$ = 0.3 V vs Ag/Ag^+) and clearly originates from the N-radical generation (Figure 4). However, the decrease of E_{Red} of the amine **1a** upon deprotonation is not sufficient for practical reaction rates. Direct anodic oxidation is still sensitive to the electrode material due to substrate-electrode surface physisorbtive interactions over the outer-sphere oxidation pathway.

Therefore, we switched to the mediated anodic oxidation and electrosynthetic mediators with E_{Red} up to 0.9 V vs Ag/Ag^+ were tested. All tertiary amines tested,[16] aminoxyl mediators,[17] and ferrocene[18] failed to support the reaction (Table 1, entries 4 and 5). Noteworthy, mediators such as TEMPO inhibited the formation of the desired product, pointing towards the radical nature of the reaction initialization. Finally, simple halide salts, also known as redox mediators,[19] were successfully tested (see SI). To be noted, electrochemical oxidations with the help of halides are known to proceed via an inner-sphere path, which is typically of several orders faster when compared to the outer-sphere one.[19] While chloride and iodide salts led to a complex mixture of products or poor current efficiencies due to concurrent oxidation/reduction, bromide anions were found to be good mediators for the electrochemical amination in undivided cells.

Based on CV, the bromide (Br^-) has two E_{Red} potentials detectable in acetonitrile on graphite, glassy carbon and platinum electrodes (Figure 5). First anodic peak is attributed to the formation of Br_3^- while the second represents the formation of Br_2. Despite same scan rates and same geometrical surface area of electrodes, the bromide oxidation current on graphite is three-fold higher due to higher active surface area. While the oxidation peak at 0.8 V vs Ag/Ag^+ shows some reversibility, the peak at E_{Red} = 0.5 V vs Ag/Ag^+ has no reductive half-wave due to fast diffusion of Br_3^- into the bulk solution.

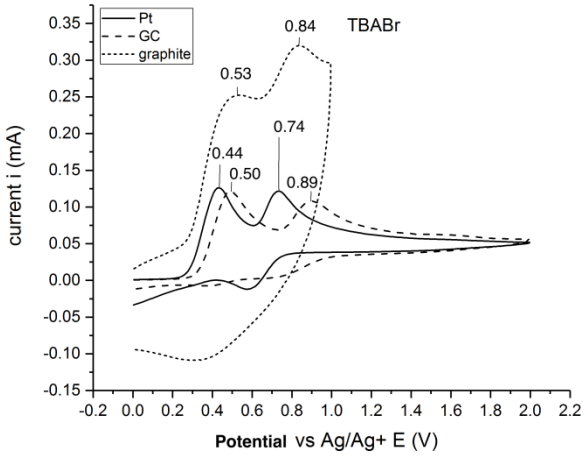

Figure 5. Cyclic voltammetry of the tetrabutylammonium bromide (5 mM in 0.1 M of Bu_4NPF_6 in CH_3CN); Work. el. 8 mm^2; Ref. el.: Ag-wire in 10 mM $AgNO_3$ / 0.1 M Bu_4NPF_6 in CH_3CN; scan rate = 100 mV/s.

When similar measurements were performed in methanol (Figure 6) the only on-set potential E_{onset} = 0.8 V vs Ag/Ag^+ was detected due to the existing base and fast formation of methyl hypobromite (MeOBr). Nevertheless, both Br_3^- and MeOBr are sufficiently reactive to oxidize the deprotonated starting material and also inert enough to prevent undesired overoxidation and Csp^2-H bromination.

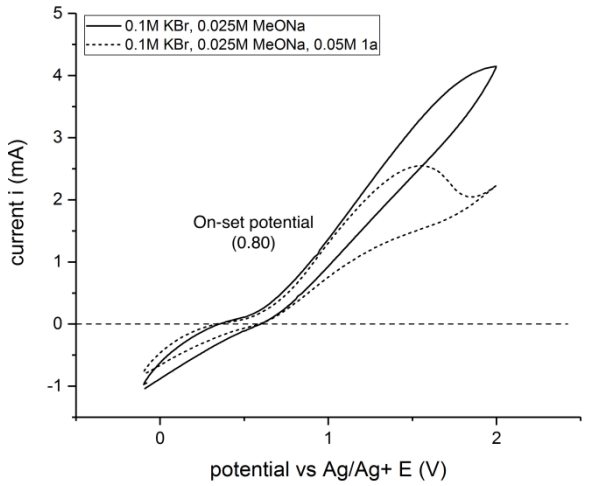

Figure 6. Cyclic voltammetry of the reaction mixture under the optimized conditions, without starting material (solid line) and with **1a** (dashed line). (50 mM in 100 mM of KBr and 25 mM of MeONa in CH_3OH); Work. el.: Graphite, 8 mm^2; Ref. el.: Ag-wire in 10 mM $AgNO_3$ / 0.1 M Bu_4NPF_6 in CH_3CN; scan rate = 100 mV/s.

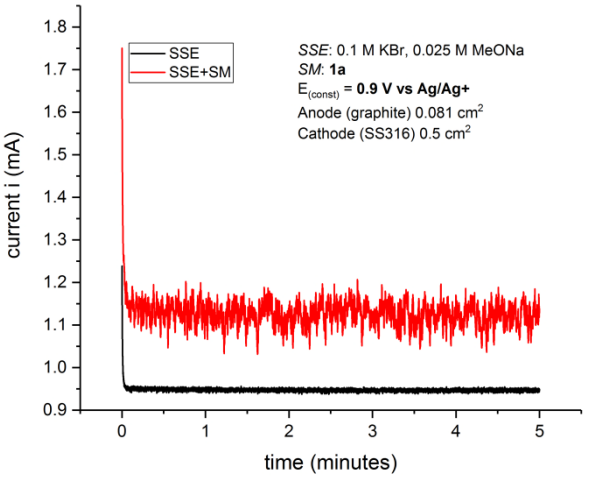

Figure 7. Chronoamperometry of the reaction mixture with **1a** (50 mM in 100 mM of KBr and 25 mM of MeONa in CH_3OH); Ref. el.: Ag-wire in 10 mM $AgNO_3$ / 0.1 M Bu_4NPF_6 in CH_3CN; Stirring rate = 500 rpm.

Chronoamperometry (CA) at the given constant potential revealed that the optimal current densities are 9.5 mA/cm^2 for the solvent/supporting electrolyte system and 11.5 mA/cm^2 for the reaction mixture (Figure 7) which are in good agreement with the optimized current density of 10 mA/cm^2. A slight increase in the current density (Figure 7) upon addition of the starting material as well as broader current fluctuations (red line) when compared to the only bromide oxidation (black line) is a clear evidence for the mediated electrochemical process.

Due to the price and availability, the corresponding alkali bromides were used as both mediator and supporting electrolyte. Subsequent variation of the reaction atmosphere, temperature and amount of light (Table 1, Entries 6-8) did not affect the reaction, and **1b** was obtained in comparable yields in all cases. Among the cathodes tested, stainless steel 316 performed the best. Various metals provided reaction outcome similar to that achieved with steel; however, titanium gave only moderate yields. Surprisingly, the pure copper cathode (Table 1, Entry 10) completely inhibited the reaction, most likely due to the high hydrogen reduction overpotential. No reaction was detected even when up to 15 F/mol of electricity was used due to the dynamic bromide oxidation/reduction equilibrium on the copper cathode. Indeed, when we recorded several cyclic voltammograms of the **1a** N-bromo-derivative (Figure 8) on different electrodes a high reduction peak was clearly visible, particularly on the copper working electrode.

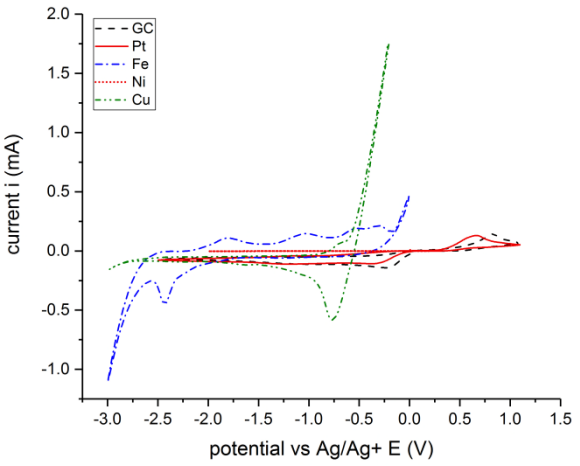

Figure 8. Cyclic voltammetry of the N-bromo-derivative of **1a** (5 mM in 0.1 M of Bu_4NPF_6 in CH_3CN); Work. el. 8 mm^2; Ref. el.: Ag-wire in 10 mM $AgNO_3$ / 0.1 M Bu_4NPF_6 in CH_3CN; scan rate = 100 mV/s.

In addition to the methanol reaction system, an acetonitrile/water mixture can also be used (Table 1, Entry 14). However, double amount of electricity (8 F/mol) was needed to obtain the desired product **1b** in decent yield.

With the optimized reaction conditions in hand, the scope of Ts-protected aliphatic amines was evaluated (Figure 9). First, various substrates **1a** - **25a**, **28a**, and **29a** bearing aromatic and heteroaromatic groups in the δ-position were subjected to the reaction conditions. Starting materials bearing both electron-donating and electron-withdrawing substituents on the aromatic ring were converted into the desired products in good yields. Pyrrolidine **11b** was isolated in only moderate yield, most likely due to the electronic effects of the ortho-fluoro substituent.

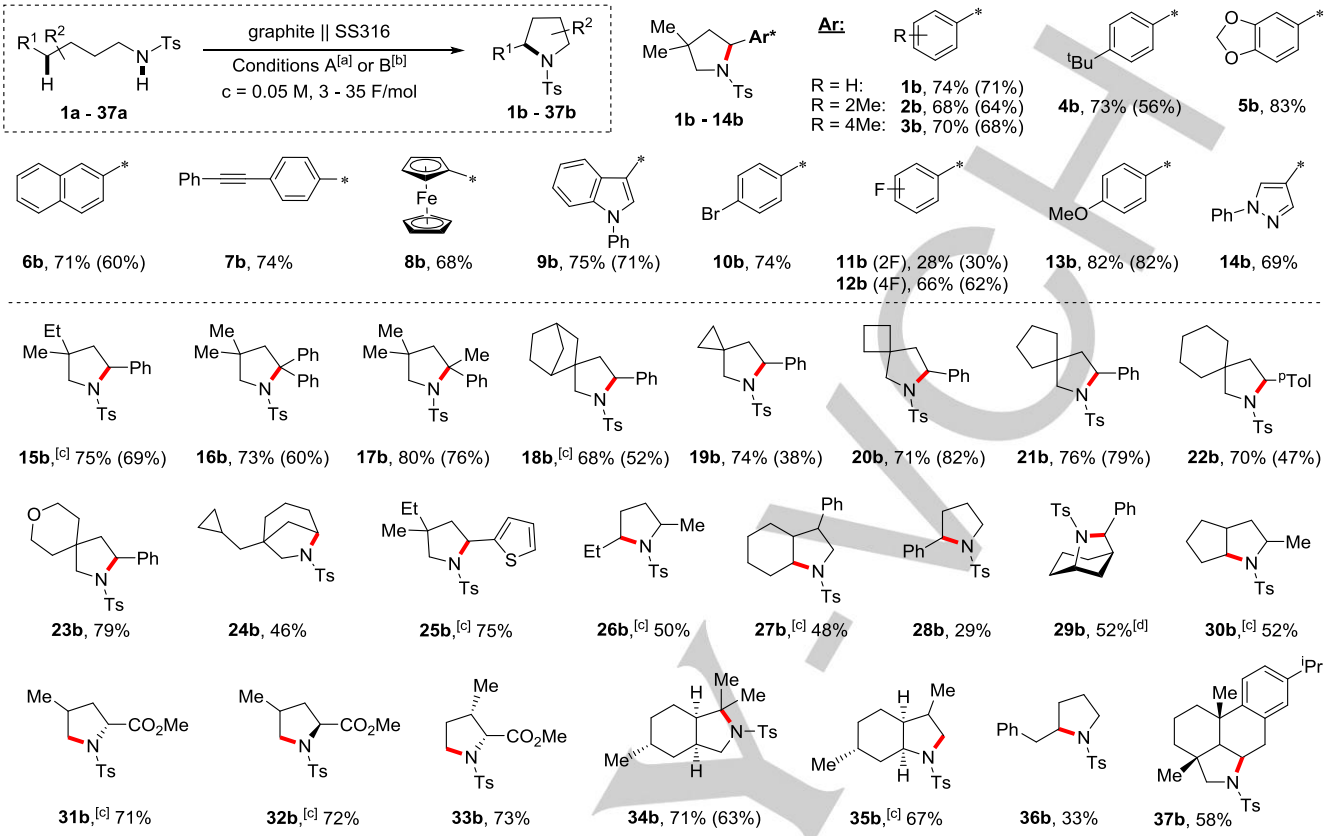

Figure 9. Scope of the Electrochemical HLF reaction of aliphatic N-tosyl-protected amines. [a] Reaction conditions: methanolic 0.1 M KBr, 0.025 M MeONa, 0.05 M substrate, graphite anode, stainless steel cathode, J = 10 mA/cm^2, Q = 3 to 35 F/mol, isolated yields. [b] For the results in brackets, the reaction conditions are as follows: methanolic 0.125 M MeONa, 0.025 M substrate, graphite anode and cathode, J = 10 mA/cm^2, Q = 3 to 35 F/mol, isolated yields. [c] Isolated as a mixture of diastereomers (ratio is close to 1:1). [d] Yields are based on recovered starting material.

Steric hindrance does not affect the reaction, as methylated products **2b** and **3b** were obtained in similar yields. Substrates bearing sensitive functional groups, such as methylenedioxy (**5a**), triple bond (**7a**) and even ferrocene (**8a**) moieties, were smoothly converted into the corresponding pyrrolidines in good yields. The reaction conditions were also suitable for substrates bearing heterocyclic groups such as indole (**9a**), pyrazole (**14a**) and thiophene (**25a**). In addition to secondary C-H bonds, tertiary bonds also underwent the electrochemical amination reaction and lead to tetra-substituted pyrrolidines **16b** and **17b** in good yields. Aza-spirocyclic compounds are valuable scaffolds in drug discovery.[20] Notably, we were able to prepare a number of saturated spiro-pyrrolidines, **18b** - **24b**, including oxygen-containing derivative **23b**, by the same strategy. Interestingly, the size of the spiro-ring did not affect the success of the reaction, and the desired pyrrolidines were obtained in good yields. Nonactivated C-H bonds reacted successfully, although a much higher amount of electricity was required. For example, during the preparation of di- and trisubstituted pyrrolidines **26b**, **27b** and **30b**, 6 to 10 F/mol electricity was required to produce the desired products in moderate yields. Furthermore, azabicyclic pyrrolidine **29b**, which is of interest in medicinal chemistry, was prepared. Such scaffolds are used as NMDA, 5HT3, and neuronal nicotinic receptor antagonists.[21] Interestingly, starting material **29a** was subjected to the reaction as a cis/trans mixture, and due to the expected conformational restrictions, only the cis-isomer underwent the reaction to give the desired product, and the trans-isomer was successfully recovered.

Mechanistically, based on CV studies and experiments, in the bromide-mediated reaction, electro-oxidation of bromide (Br^-) leads to the formation of bromine (Br_2) active species, which is immediately trapped by excess bromide to generate Br_3^- anion and consequently converted to methyl hypobromite (MeOBr).[22] Due to the low potential (0.3–0.8 V vs Ag/Ag$^+$), only N-bromo species **B** can be generated at the electrode, which forms N-centered radical **A** either by light-supported homolytic cleavage or by a SET event on the cathode (Scheme 2). Compound **A** is converted to C–centered radical **C** via a 1,5-HAT process through a 6-membered cyclic transition state.

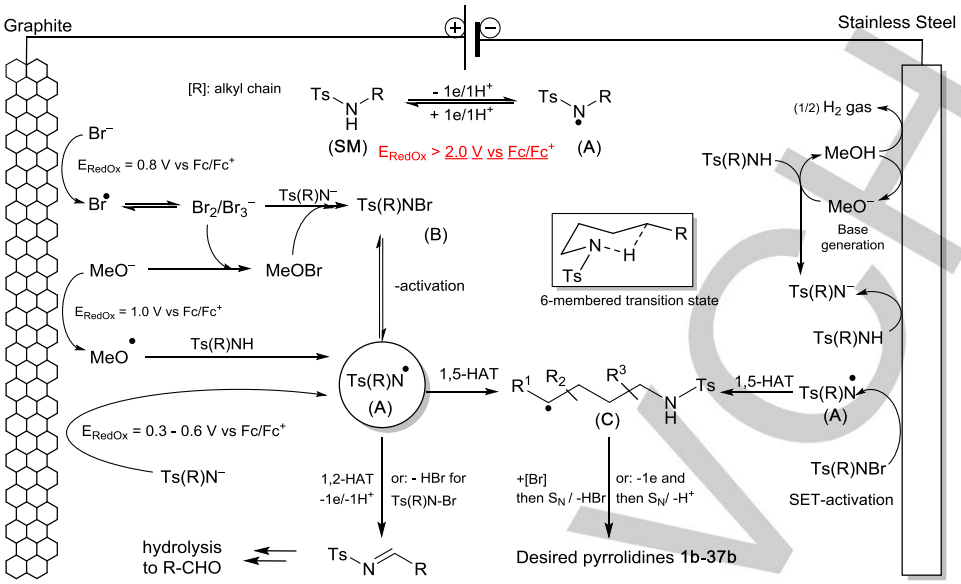

Scheme 2. Proposed mechanism for the electrochemical C(sp^3)-H amination.

Although such radicals are believed to be quenched by N-Br or MeOBr species, similar to the reported photoredox processes,[23] we could neither detect nor isolate the corresponding alkyl bromide due to the rapid S_N step. In the direct halogen-free, oxidative process, radical **C** is believed to be oxidized to a carbocation while it is physisorbed onto the surface of the electrode. In both cases, the formation of pyrrolidine is achieved by nucleophilic substitution with the N-H group. In addition to the 1,5-HAT reaction, α-deprotonation of N-Br intermediate **B** is observed with formation of the corresponding aldimine (RCH=NTs) followed by hydrolysis to the corresponding aldehyde. The chemoselectivity is typically dependent on the molecular conformation and BDE of the reacting C-H bond.[25]

The essential role of the cathodically generated base for the reported transformation was confirmed by divided cell experiments (see SI) along with the visual observation of the evolution of molecular hydrogen (H_2). Although the starting material can be deprotonated directly at the cathode, methanol or residual water are considered the main source of the base due to the matching of the pKa value to the acidic N-H bond of the starting material. Most of the reactions to explore the substrate scope were performed in a two-electrode cell with a loading of 1-2 mmol. However, to further extend the utility of the electrochemical HLF reaction, additional scalability tests were conducted (Figure 10).

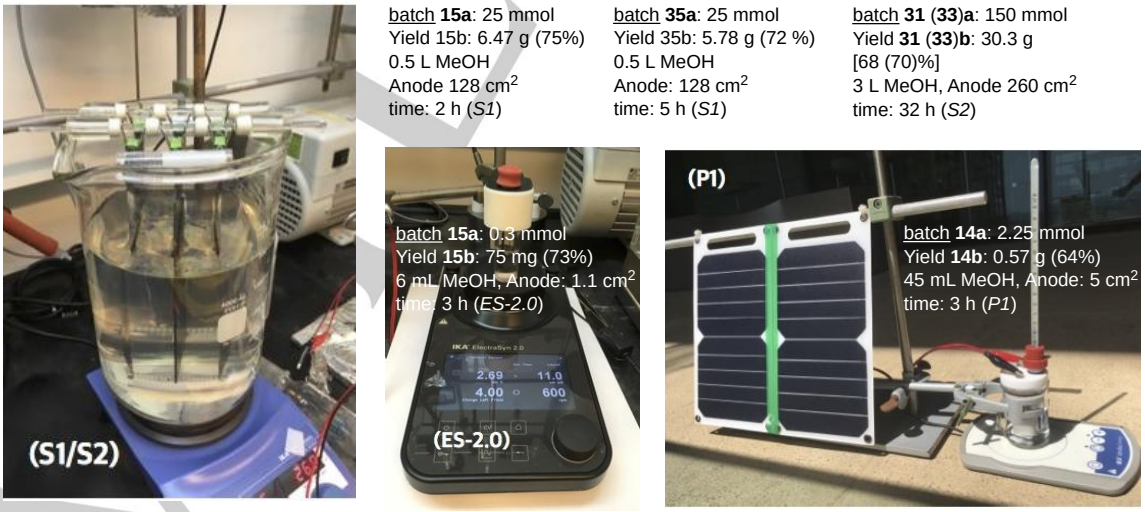

Figure 10. Scaling up of the HLF reaction. (*S1/S2*) Scaling up of the HLF reaction with **15a**, **31a**, **33a** and **35a** in batch reactions (up to 50 g loading); (*ES-2.0*) test of reproducibility with an IKA ElectroSynth system; (*P1*) Employment of a photovoltaic-powered setup

Thus, benzylic substrate **15a** and menthol-derivative **35a** were converted into the desired pyrrolidines in 75 and 72% yields after 2 and 5 hours, respectively. Almost no differences, except for a much lower current efficiency, were observed even in the 50-g scale cyclizations of protected amino acids such as leucine and isoleucine to the corresponding 4- and 3-methyl proline carboxylates (Figure 10 *S1*/*S2*). To our delight, desired products **31b** and **33b** were isolated in 68 and 70% yield, while unreacted starting material and pyrrolidinin-2-one-carboxylates accounted for the remaining mass balance. Concerning the amount of electricity used, the solvent and the chemicals (isoleucine: 2 $/g, Acros), the production cost of highly valuable enantiopure methyl N-tosyl-3-methyl-proline carboxylate (**33b**, 705 $/g, Acros) from the corresponding protected amino acid can be estimated as only 100 $ per 1 mol.

A recently launched commercially available electrosynthesizer (by IKA, Figure 4, *ES-2.0*)[24] was applied to evaluate the reproducibility of the reaction. Products **7b**, **15b**, and **23b** were all obtained in similar chemical and faradaic yields. Photovoltaic panels were tested as an alternative source of electricity in the synthesis of **14b** (Figure 4, *P1*). The reaction outcome did not change compared to that achieved using the conventional electrical network. Notably, due to the outdoor ambient temperature, the reaction mixture was heated to 50 °C regardless of if it was exposed to direct sunlight or kept in shadow. Nevertheless, the desired pyrazole-substituted pyrrolidine was isolated in 64% yield.

Further scaling up of the reaction by employing a continuous flow setup (Table 2) was also examined. For the optimization of the reaction conditions the Asia Syrris® flow reactor was employed.

Table 2. Optimization of the reaction conditions under continuous flow.[a]

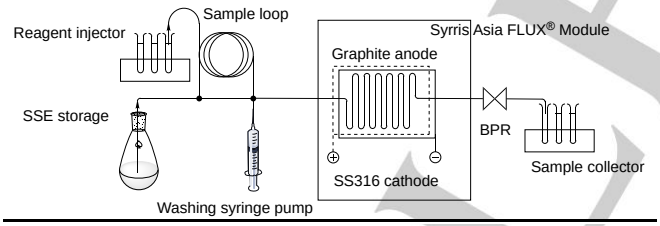

Entry	Mode [b]	Flow rate (µL/min)	Back pressure (bar)	Conversion/ Yield (%)[c]
1	CV (3.5 V)	250	1	28/24
2	CV (3.5 V)	250	2	36/31
3	CV (3.0 V)	250	3	54/48
4	CV (2.8 V)	125	4	67/60
5	CV (2.8 V)	125	5	84/76[d]
6	CC (5 mA/cm^2)	125	5	85/75

[a] Reactions were conducted with stock solution of 0.025 M KBr, 0.0125 M MeONa, and 0.05 M starting material in methanol, *SSE* is a solvent/supporting electrolyte, *BPR* – back pressure regulator. [b] *Mode* refers to the constant voltage (CV) in volts or constant current (CC) and current density (J) respectively. [c] Conversion and yields are based on GC-FID. [d] Conversion is based on recovered starting material; Yield is isolated after column chromatography.

The flow setup contains methanolic electrolyte solution feed followed by the sample loop connected to the reagent injector. The electrochemical cell with a graphite anode and an SS 316 cathode equipped with a Teflon® separating gasket has an internal volume of 225 µL and 12 cm^2 of total surface area. Over the course of the reaction, due to release of hydrogen and the closed system the general liquid flow was unevenly cut into small slugs of different size. Such phenomenon significantly increases the overall flow rate due to the difference in viscosity and at normal pressure we completely failed to achieve conversions above 20% even at the slowest flow rate possible (10 µL/min). The usage of other cathodes which might produce less hydrogen such as graphite or tin didn't solve the problem either. Decreasing the temperature usually increases the solubility of the gases, however, in our case it decreased also the reaction rate and the conversions were again low. Finally, the general pressure in the system was increased with the help of a back pressure regulator. To our delight, the conversion as well as the yield gradually increased with the pressure applied in the range from 1 to 5 bars (Table 2, Entries 1-5). Nevertheless, fluidic slugs of hydrogen gas were still detectable, but the number of bubbles was drastically reduced providing quasi-even flow over the channels in the cell. Eventually, tuning of the flow rate and the applied voltage provided us the optimal conditions for the electrochemical C(sp^3)-H amination under continuous flow conditions (Table 2, Entries 5 and 6) for both constant voltage and constant current modes.

Finally, 250 mL of the methanolic stock solution of butylamine **15a** was pumped through the flow cell over 34 h without significant changes in the reactivity. The desired pyrrolidine **15b** was isolated in 76% yield with 16% of the starting material being recovered.

Conclusions

In conclusion, we have developed a sustainable and environmentally benign protocol for an electrochemically driven, intramolecular direct C(sp^3)-H amination.[26] Transition-metal catalysts and/or (super)stoichiometric oxidants were successfully replaced by "traceless" anodic oxidation. The electrochemical reaction utilizes an industrially acceptable solvent-supporting electrolyte system and inexpensive graphite and stainless-steel electrodes. Furthermore, we applied this method to both direct and mediated electrochemical reactions. The developed reaction conditions were compatible with a wide variety of functional groups, and the desired pyrrolidines were obtained with great regioselectivity, good yields and reasonable current efficiency. The amount of electricity required was correlated with the BDE of the corresponding C(sp^3)-H bonds. The anodic transformations of Ts-*iso*Leu-OMe and Ts-Leu-OMe to the methyl-substituted proline methyl esters were efficiently performed on a 50-g scale; therefore, the protocol can be implemented for large-scale synthetic applications.

Experimental Section

The following procedure is representative for the electrochemical preparation of the N-tosyl-protected pyrrolidines:

A cell equipped with a stirring bar was loaded with 0.2 mmol of N-tosyl alkylamine followed by 4 mL of 0.1 M KBr in methanol with 0.025 M NaOMe. The reaction vial was closed with a lid equipped with 2 electrodes (2 cm × 0.7 cm each). The electrodes were adjusted to allow for the normal spinning of the stirring bar, to be immersed in liquid at 1.5 cm to generate a surface area of approximately 1 cm^2, and to constantly be separated by 0.6 cm. The stirring rates were set to be from 600 to 1000 rpm to facilitate proper mass transfer during the electrolysis. Stirring too quickly must be avoided to prevent vortex formation, which may change the actual surface area of the electrodes. For the halogen-free reaction, 2 graphite plates were used as electrodes and 4 mL of 0.125 M NaOMe in methanol solution were used for 0.1 mmol of starting material. The power supply was connected, and the reaction mixture was electrolyzed under a constant current (J = 10 mA/cm^2). The reaction progression was monitored by TLC or GC-MS after the theoretically required amount of electricity had passed (2 F/mol) and then after every 1 F/mol until full conversion was reached. After the reaction was completed, the mixture was transferred via syringe to a 25-mL RB flask, the electrodes were washed with methanol, and the combined solvents were removed in vacuo. The residue was redissolved in DCM, 4 g of silica was added, and the solvent was carefully removed again to afford a free-flowing powder, which was directly purified by column chromatography. Additional experimental details are provided in the Supplemental Information.

Keywords: Amination • Electrosynthesis • 1,5-HAT • pyrrolidines • flow electrolysis

[1] a) *Hydrogen-Transfer Reactions* (Eds.: J. T. Hynes, J. P. Klinman, H.-H. Limbach, R. L. Schowen), Wiley-VCH, Weinheim, **2007**; b) M. Nechab, S. Mondal, M. P. Bertrand, *Chem. Eur. J.* **2014**, *20*, 16034; c) L. Capaldo, D. Ravelli, *Eur. J. Org. Chem*. **2017**, 2056; d) X.-Q. Hu, J.-R. Chen, W.-J. Xiao, *Angew. Chem. Int. Ed*. **2017**, *56*, 1960; e) L. M. Stateman, K. M. Nakafuku, D. A. Nagib, *Synthesis* **2018**, *50*, 1569.

[2] *Encyclopedia of Radicals in Chemistry, Biology and Materials* (Eds.: C. Chatgilialoglu, A. Studer), John Wiley & Sons, Ltd., Chichester, **2012**.

[3] a) A. Popelak, G. Lettenbauer, in *The Alkaloids: Chemistry and Physiology*, *Vol. 9* (Ed.: R. H. F. Manske), Academic Press: New York, **1967**, pp. 467 – 482; b) K. Kawanishi, Y. Uhara, Y. Hashimoto, *J. Nat. Prod.* **1982**, *45*, 637; c) S. F. Martin, in *The Alkaloids: Chemistry and Pharmacology*, *Vol. 30* (Ed. A. Brossi) Academic Press, New York, **1987**, pp. 251 – 376; d) E. Fattorusso, O. Taglialatela-Scafati, *Modern Alkaloids*, (Eds.: E. Fattorusso, O. Taglialatela-Scafati) Wiley-VCH, Weinheim, **2007**; e) R. F. George, N. S. M. Ismail, J. Stawinski, A. S. Girgis, *Eur. J. Med. Chem*. **2013**, *68*, 339; f) C. Bhat, *Chemistry Open*. **2015**, *4*, 192; g) Á. A. Kelemen, G. Satala, A. J. Bojarski, G. M. Keserű, *Molecules* **2017**, *22*, 2221.

[4] a) C. B. Burness, *Drugs* **2015**, *75*, 1947; b) J. Y. L. Chung, J. P. Scott, C. Anderson, B. Bishop, N. Bremeyer, Y. Cao, Q. Chen, R. Dunn, A. Kassim, D. Lieberman, A. J. Moment, F. Sheen, M. Zacuto, *Org. Process Res. Dev.* **2015**, *19*, 1760; c) N. Ashousha, *Pharma Chemica* **2016**, *8*, 292; d) R. A. Duffy, C. Morgan, R. Naylor, G. A. Higgins, G. B. Varty, J. E. Lachowicz, E. M. Parker, *Pharmacol. Biochem. Behav*. **2012**, *102*, 95; e) Y.-A. Heo, E. D. Deeks, *Drugs* **2017**, *77*, 1687.

[5] A. C. Flick, H. X. Ding, C. A. Leverett, S. J. Fink, C. J. O'Donnel, *J. Med. Chem*. **2018**, *61*, 7004.

[6] a) A. W. Hofmann, *Ber. Dtsch. Chem. Ges.* **1883**, *16*, 558; b) A. W. Hofmann, *Ber. Dtsch. Chem. Ges.* **1885**, *18*, 5; c) A. W. Hofmann, *Ber. Dtsch. Chem. Ges.* **1885**, *18*, 109; d) K. Löffler, C. Freytag, *Ber. Dtsch. Chem. Ges.* **1909**, *42*, 3427.

[7] a) Manfred E. Wolff, *Chem. Rev*. **1963**, *63*, 55; b) G. Majetich, K. Wheless, *Tetrahedron* **1995**, *51*, 7095; c) X.-Q. Hu, J.-R. Chen, W.-J. Xiao, *Angew. Chem. Int. Ed*. **2017**, *56*, 2.

[8] a) R. Hernández, A. Rivera, J. A. Salazar, E. Suárez, *J. Chem. Soc. Chem. Commun.* **1980**, 958; b) C. Betancor, J. I. Concepción, R. Hernández, J. A. Salazar, E. Suárez, *J. Org. Chem.* **1983**, *48*, 4430.

[9] a) P. DeArmas, R. Carrau, J. L. Concepción, C. G. Francisco, R. Hernández, E. Suárez, *Tetrahedron Lett.* **1985**, *26*, 2493; For related protocols, see: b) R. Carrau, R. Hernández, E. Suárez, C. Betancor, *J. Chem. Soc. Perkin Trans. 1* **1987**, 937; c) P. De Armas, C. G. Francisco, R. Hernández, J. A. Salazar, E. Suárez, *J. Chem. Soc. Perkin Trans. 1* **1988**, 3255; d) C. G. Francisco, A. J. Herrera, E. Suárez *J. Org. Chem.* **2003**, *68*, 1012; e) A. Martín, I. Pérez-Martín, E. Suárez; *Tetrahedron* **2009**, *65*, 6147; f) R. Fan, D. Pu, F. Wen, J. Wu, *J. Org. Chem.* **2007**, *72*, 8994.

[10] a) C. Martínez, K. Muñiz, *Angew. Chem. Int. Ed.* **2015**, *54*, 8287; For related protocols, see: b) N. R. Paz, D. Rodríguez-Sosa, H. Valdés, R. Marticorena, D. Melián, M. B. Copano, C. C. González, A. J. Herrera, *Org. Lett.* **2015**, *17*, 2370; c) C. Q. O'Broin, P. Fernández, C. Martínez, K. Muñiz, *Org. Lett.* **2016**, *18*, 436; d) P. Becker, T. Duhamel, J. C. Stein, M. Reiher, K. Muñiz, *Angew. Chem. Int. Ed.* **2017**, *56*, 8004; e) P. Becker, T. Duhamel, C. Martínez, K. Muñiz, *Angew. Chem. Int. Ed.* **2018**, *57*, 5166.

[11] E. A. Wappes, S. C. Fosu, T. C. Chopko, D. A. Nagib, *Angew. Chem. Int. Ed.* **2016**, *55*, 9974.

[12] a) O. R. Luca, J. L. Gustafson, S. M. Maddox, A. Q. Fenwick, D. C. Smith, *Org. Chem. Front.* **2015**, *2*, 823; b) *Organic Electrochemistry*, 5th Edition (Eds.: O. Hammerich, B. Speiser), CRC Press, Boca Raton, **2015**; c) E. J. Horn, B. R. Rosen, P. S. Baran, *ACS Cent. Sci.* **2016**, *2*, 302; d) M. Yan, Y. Kawamata, P. S. Baran, *Chem. Rev.* **2017**, *117*, 13230; e) Y. Jiang, K. Xu, C. Zeng, *Chem. Rev.* **2018**, *118*, 4485; f) S. Möhle, M. Zirbes, E. Rodrigo, T. Gieshoff, A. Wiebe, S. R. Waldvogel, *Angew. Chem. Int. Ed*. **2018**, *57*, 6018; g) A. Wiebe, T. Gieshoff, S. Möhle, E. Rodrigo, M. Zirbes, S. R. Waldvogel, *Angew. Chem. Int. Ed*. **2018**, *57*, 5594; f) K. Mitsudo, Y. Kurimoto, K. Yoshioka, S. Suga, *Chem. Rev.* **2018**, *118*, 5985.

[13] a) J. H. Wagenknecht, *J. Chem. Educ.* **1983**, *60,* 271; b) D. S. P. Cardoso, B. Šljukić, D. M. F. Santos, C. A. C. Sequeira, *Org. Process Res. Dev.* **2017**, *21*, 1213.

[14] For examples, see: a) T. Shono, Y. Matsumura, S. Katoh, K. Takeuchi, K. Sasaki, T. Kamada, R. Shimizu, *J. Am. Chem. Soc.*, **1990**, *112*, 2368; b) H.-C. Xu, J. M. Campbell, K. D. Moeller; *J. Org. Chem.* **2014**, *79*, 379; c) L. Zhu, P. Xiong, Z.-Y. Mao, Y.-H. Wang, X. Yan, X. Lu, H.-C. Xu, *Angew. Chem. Int. Ed.* **2016**, *55*, 2226; d) S. Zhang, L. Li, M. Xue, R. Zhang, K. Xu, C. Zeng, *Org. Lett.* **2018**, *20*, 3443; e) Z.-W. Hou, Z.-Y. Mao, Y. Y. Melcamu, X. Lu, H.-C. Xu *Angew. Chem. Int. Ed.* **2018**, *57*, 1636; f) T. Gieshoff, A. Kehl, D. Schollmeyer, K. D. Moeller, S. R. Waldvogel, *Chem. Commun.*, **2017**, *53*, 2974; g) T. Gieshoff, A. Kehl, D. Schollmeyer, K. D. Moeller, S. R. Waldvogel, *J. Am. Chem. Soc*. **2017**, *139*, 12317; h) T. Gieshoff, D. Schollmeyer, S. R. Waldvogel, *Angew. Chem. Int. Ed.*, **2016**, *55*, 9437.

[15] a) P. T. Anastas, J. C. Warner in *Green Chemistry: Theory and Practice* (Oxford Univ. Press) **1998**; b) F. P. Byrne, S. Jin, G. Paggiola, T. H. M. Petchey, J. H. Clark, T. J. Farmer, A. J. Hunt, C. R. McElroy, J. Sherwood, *Sustain. Chem. Process* **2016**, *4*:7.

[16] S. F. Nelsen, P. J. Hintz, *J. Am. Chem. Soc.* **1972**, *94,* 7114.

[17] For selected examples, see: a) A. Deronzier, D. Limosin, J.-C. Moutet, *Electrochim. Acta* **1987**, *32,* 1643; b) K. Schnatbaum, H.-J. Schäfer, *Synthesis* **1999**, *5*, 864; c) E. M. Belgsir, H.-J. Schäfer, *Electrochem. Commun.* **2001**, *3,* 32; d) D. Liaigre, T. Breton, E. M. Belgsir, *Electrochem. Commun.* **2005**, *7*, 312; e) E. J. Horn, B. R. Rosen, Y. Chen, J. Tang, K. Chen, M. D. Eastgate, P. S. Baran, *Nature* **2016**, *533*, 77.

[18] For selected examples, see: a) P. Xiong, H.-H. Xu, J. Song, H.-C. Xu, *J. Am. Chem. Soc.* **2018**, *140*, 2460; b) Z.-W. Hou, Z.-Y. Mao, J. Song, H.-C. Xu, *ACS Catal.* **2017**, *7,* 5810; c) Z.-W. Hou, Z.-Y. Mao, H.-B. Zhao, Y. Y. Melcamu, X. Lu, J. Song, H.-C. Xu, *Angew. Chem. Int. Ed.* **2016**, *55*, 9168; d) Z.-J. Wu, H.-C. Xu, *Angew. Chem. Int. Ed.* **2017**, *56*, 4734; e) Z.-J. Wu, S.-R. Li, H. Long, H.-C. Xu, *Chem. Commun.* **2018**, *54*, 4601.

[19] a) E. Steckhan, *Top. Curr. Chem.* **1987**, *142*, 1; b) E. Steckhan, *Angew. Chem., Int. Ed.* **1986**, *25*, 683 and the references cited therein.

[20] G. Meller, T. Berkenbosch, J. C. J. Benningshof, D. Stumpfe, J. Bajorath, *Chem. Eur. J.* **2017**, *23*, 703.

[21] C. Parsons, W. Danysz, M. Gold, I. Kalvinsh, V. Kauss, A. Jirgensons, *US2007105961*, **2007**.

[22] T. ‐ L. Ho, M. Fieser, L. Fieser in *Fiesers' Reagents for Organic Syntheses*, **1975**, *5*, 446.

[23] M: D. Kärkäs; *ACS Catal.* **2017**, 7, 4999-5022 and references cited therein.

[24] S. J. Blanksby, G. B. Ellison, *Acc. Chem. Res.* **2003**, *36*, 255.

[25] M. Yan, Y. Kawamata, P. S. Baran, *Angew. Chem. Int. Ed*. **2018**, *57*, 4149.

[26] During the preparation of this manuscript a similar protocol was reported: a) S. Herold, D. Bafaluy, K. Muñiz, *Green Chem*. **2018**, *20*, 3191; b) X. Hu, G. Zhang, F. Bu, L. Nie, A. Lei, *ACS Catal*. **2018**, *8*, 9370.

10.1002/chem.201806092

WILEY-VCH

Layout 2:

FULL PAPER

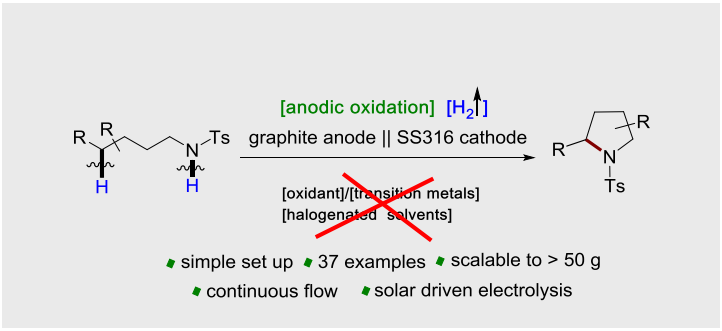

*Pavlo Nikolaienko, Marc Jentsch, Ajit P. Kale and Magnus Rueping**

Page No. – Page No.

Electrochemical and scalable dehydrogenative C(sp^3)-H amination via remote hydrogen atom transfer in batch and continuous flow